Optical and Quantum Electronics (2023) 55:113
https://doi.org/10.1007/s11082-022-04450-9

Mixed line broadening in the saturable absorption of erbium-doped fiber

Deeksha Jachpure[1] · **R. Vijaya**[1,2]

Received: 12 August 2022 / Accepted: 30 November 2022 / Published online: 17 December 2022

Abstract
Measuring the absorption coefficient and analyzing the saturable absorption property of erbium-doped fiber (EDF) of different lengths at different values of input power is necessary for designing amplifiers and lasers with optimum features. Absorption coefficient for shorter lengths such as 1 m results in a perfect match between the experimentally obtained data and the trend expected for a homogeneously broadened system. This was not the case for longer lengths such as 4.6 m, 11 m and 25 m of EDF. The characteristic equation for saturable absorption needs modification at longer lengths of EDF. The deviation in the trend, from systems with homogeneous and inhomogeneous broadening, is very systematic with an increase in fiber length, input power and the operating wavelength. The influence of an increase in these three factors is similar, with a larger deviation from the standard inhomogeneous case to an increased inhomogeneity. The characteristics of saturable absorption in the presence of another signal at a lower wavelength imply a more rapid deviation from inhomogeneous broadening, but towards homogeneous broadening.

Keywords Saturable absorption · Erbium-doped fiber · Homogeneous and inhomogeneous broadening

1 Introduction

Erbium-doped fiber (EDF) has been an integral part of the fiber-based optical systems since the 1990s. It has been studied extensively for its performance characteristics over the years (Ainslie 1991; Becker et al. 1999; Desurvire 2002; Giles and Desurvire 1991; Harun et al. 2007; Kang et al. 2012). As a result, it is deployed extensively in commercial use, becoming an essential component present within the optical amplifiers of today's optical communication links. Apart from its most well-known commercial application in optical amplifiers, EDF in lasers has been studied for tunability, broad-band output, ultrashort pulses, coherence characteristics, chaotic output, bistable characteristics, high-power possibilities, and multi-wavelength lasing (Bellemare 2003; Bradley and Pollnau 2011; Digonnet 1993;

✉ R. Vijaya
rvijaya@iitk.ac.in

[1] Centre for Lasers and Photonics, Indian Institute of Technology Kanpur, Kanpur 208016, India

[2] Department of Physics, Indian Institute of Technology Kanpur, Kanpur 208016, India

Li et al. 2021; Suchita and Vijaya 2017). In these studies, different lengths of EDF have been used as suitable to each application. In spite of the vast amount of reported research on EDF, some of its properties are not fully explored, partly because it is a highly complex system (Desurvire 2002) as well as because it is subject to fabrication conditions, doping concentration levels and spatial inhomogeneity of the dopants. One such property is whether it has a homogeneous or an inhomogeneous or a mixed broadening in its line shape, and how this aspect may influence some of its applications.

Homogeneous broadening is the consequence of natural line-broadening mechanisms. Stark splitting of the levels in EDF is not homogeneous; but, the Stark-split sub-levels have very small differences in energy and are therefore strongly coupled by the effect of thermalization at room temperature in EDF (Desurvire 2002). This is expected to lead to homogeneous broadening of the line shape. In doped glasses at room temperature, which includes the EDF used in amplifiers and lasers, site-to-site variations can induce strain broadening and may increase the role of inhomogeneous broadening (Siegman 1986). In fact, radiative transitions can be strongly homogeneous or strongly inhomogeneous or even somewhere in between for doped glasses (Siegman 1986). There can be other factors that contribute as well, and the role of homogeneous and inhomogeneous broadening can manifest differently in different designs. For example, the length of the active medium and the resonator design decide the number of longitudinal modes in a laser; in EDF-based laser designs that employ multiple longitudinal modes, inhomogeneity has been reported (Deepa and Vijaya 2007). For a complex material system such as the EDF, categorizing it as only homogeneously or only inhomogeneously broadened may not be valid. Mixed broadening was extensively studied in semiconductor lasers in the 1970s and 1980s, and led to several improvements in commercial designs (Casperson 1981, 1987). Our work indicates the importance of understanding this mechanism in EDF-based lasers and amplifiers.

In our recent work, we studied the process of saturable absorption in EDF through an extensive set of measurements to quantify its role in absorptive optical bistability (Jachpure and Vijaya 2022). As its extension, we analyze here some more aspects of saturable absorption in EDF, such as whether the saturable absorption is that of a purely homogeneously or inhomogeneously broadened transition and if it has a dependence on its length, and how the presence of an additional signal affects this property. While the answers to these questions are extremely important in applications where short/long EDF is used (Ge et al. 2018; Jachpure and Vijaya 2022; Li et al. 2017) and/or multiple signals could coexist and experience gain/loss, such as in EDF-based amplifiers/lasers, these have not been explored through suitable measurements, to the best of our knowledge. We study the quantitative aspects of the absorption coefficient of EDF in short and long lengths of the fiber, at different wavelengths in the C-band, and at different input power levels. In addition, we analyze its properties in the presence of another signal. This is because absorptive optical bistability has been studied earlier with a control laser in EDF-based lasers (Ge et al. 2018; Li et al. 2017). The wavelength and power of a control laser signal can affect the bistability dramatically by modifying its threshold while increasing the input power, and thus the bistable width.

The prime motivation of this work is to discuss why the effect of EDF is very different at short and long lengths, and in the presence and absence of other signals. Moreover, we aim to clarify why the earlier published work variously refers to EDF as being homogeneously broadened or inhomogeneously broadened in different experiments. There seems to be no published work (in our view) which indicates that this categorization has a dependency on EDF length (as well as the presence of an additional signal) and input power, and demonstrates those effects. Towards these objectives, we measured the transmitted power from

EDF for a wide range of input powers, from different lengths of EDF with no change in glass composition. Then, we extracted the absorption coefficient from these measurements and analyzed its trend for short and long lengths of EDF individually at different powers. This methodology has been adopted because standard propagation models in EDF will not show the trends seen in the experiment because saturable absorption is not included in them. The experiment brings out the effects in different conditions as it happens, and does not extrapolate the results from one condition to the other. Our method of measuring first and then fitting the piece-wise trends to a simple model indicates that inhomogeneities are manifest when the EDF length is not as short as a couple of meters.

We also studied the trend in the presence of another signal at two different power levels. Thus, we establish that there is a modification in the basic property of the active fiber upon increasing its length up to several meters, and the presence of another signal affects the saturable absorption of EDF differently at short/long lengths. While the use of long length of EDF in a cavity configuration leads to interesting phenomena such as the bistability (Jachpure and Vijaya 2022), and knowing its effects are essential for the accuracy and optimization of the desired results, the application of our analysis can have far-reaching consequences. For example, on the one hand, it is reported that to get multiwavelength lasing operation in an EDF laser (with EDF lengths of 50 cm, 100 cm, and 2 m), inhomogeneous broadening is necessary, and therefore homogeneous broadening is to be suppressed (An et al. 1999; Cai and Liao 2020; Zhao et al. 2021); on the other hand, it is reported that for the wavelength division multiplexed and amplifier applications with EDF (with an EDF length of 15.5 m for C-band and 77 m for L-band), homogeneous broadening has to dominate because inhomogeneous broadening distorts the EDF amplifier gain spectrum (Flood 2000; Laurent et al. 2001; Liu et al. 1999). These indicate that the dominant line broadening mechanism has an immense influence on the performance of commercial products made with widely different lengths of the EDF. Apart from the fact that our work demonstrates that the EDF behaves very differently at different lengths/powers/wavelengths, as known from multiple earlier reports, it is also to emphasize that EDF requires more in-depth and precise modelling to account for its saturable absorption during its device performance.

2 Theoretical background

EDF is an excellent absorber in the absence of any pump (Mao and Lit 2002). At sufficiently high input powers P, the absorption coefficient α of EDF shows the very interesting property of saturable absorption. The characteristic of saturable absorption in a *homogeneously* broadened system is governed by the following equation (Huang et al. 2021; Ismail et al. 2021; Zhou et al. 2019)

$$\alpha(I) = \frac{\alpha_o}{1 + \frac{I}{I_{sat}}} + \alpha_{NS} \tag{1}$$

where the linear or low-intensity absorption coefficient is α_0, the input intensity is I, and the saturation intensity is I_{sat} (which is the value of input intensity that gives $\alpha = \alpha_0/2 + \alpha_{NS}$). Here, α_{NS} is the non-saturable and intensity-independent part of the absorption coefficient, while the first term is the saturable part. This Eq. (1) is applicable for the saturation of a *homogeneously* broadened system, where the system saturates at all the wavelengths in the same way while maintaining the profile of the absorption/gain spectrum; only the

magnitude is changed. For the case of saturable absorption in an *inhomogeneously* broadened transition, where there is a change in the spectral profile, there is a modification in the equation for intensity-dependent α as (Anderson and Boffard 2017)

$$\alpha(I) = \frac{\alpha_o}{\sqrt{\left(1 + \frac{I}{I'_{sat}}\right)}} + \alpha_{NS} \tag{2}$$

Here I'_{sat} is the saturation intensity at the center frequency of the transition (emission band). This indicates that the inhomogeneous system saturates for higher input in comparison with the homogeneous system, as a function of input intensity (Anderson and Boffard 2017) as the value of I'_{sat} will be calculated through $\alpha = \alpha_0/\sqrt{2} + \alpha_{NS}$ in this case. It may be noted that Eqs. (1–2) are also applicable for powers P and P_{sat} (P'_{sat}) in the place of I and I_{sat} (I'_{sat}). In the following sections, we will analyze if the property of saturable absorption in EDF follows the features of a homogeneously or an inhomogeneously broadened system based on our power-dependent absorption measurements with different lengths of EDF. This will help us to analyze the changes in the system behavior, if any, by using the same medium and merely changing its length. Then, we study how the behaviour of saturable absorption in EDF gets altered in the presence of another signal, and based on its power. This will aid in applications where there is a need for user-defined controlled absorption by the EDF.

3 Absorption coefficient as a function of input power

The schematic of the experimental setup shown in Fig. 1a is used for carrying out the power-dependent absorption measurements in EDF at different wavelengths. A CW laser tunable in the wavelength range of 1540–1565 nm, with variable output power (Yenista OSICS mainframe) available through a single-moded fiber is used at the input to the EDF. A fixed attenuator is used to widen the range of powers available at the input of the EDF. The widest possible range is required to establish the dependence of absorption on the input power (or intensity) in an unambiguous manner. The input power (P_{in}) and the output power (P_{out}) from the EDF are measured at different input wavelengths using a fiber-coupled sensor connected to a power meter (Ophir PD300 sensor and Nova-II meter). The measured output power is used to calculate the absorption coefficient (Jachpure and Vijaya 2022). We also compared the absorption coefficient extracted from the measurements using a power meter and from an optical spectrum analyzer (OSA) (EXFO FTB 200). Both are used in our studies, and we found that the trends are very similar in both of them for input powers greater than − 30 dBm.

3.1 Short length of EDF

In this case, EDF (Fibercore, M-5) with a fixed dopant concentration of 1.405×10^{25} ions/m^3 and length of 1 m is used for performing the experiment. The black square symbols in Fig. 1b, c show the variation of absorption coefficient (in dB/m) as a function of input power at 1540 nm and 1565 nm, respectively. When the input power is very low, the small-signal absorption coefficient has a constant value. From Eqs. (1, 2), this corresponds to $\alpha_0 + \alpha_{NS}$ which is independent of power. Then it is seen to reduce

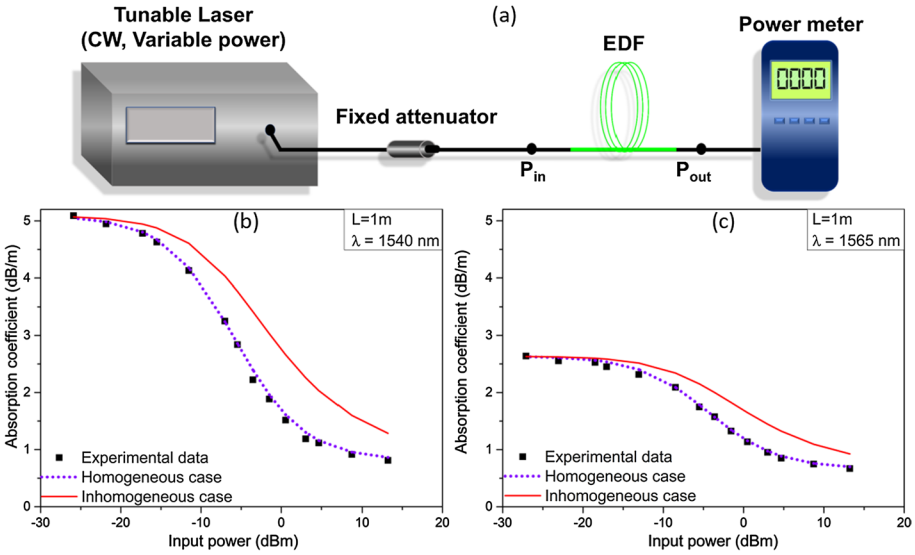

Fig. 1 **a** Schematic of the experimental setup. Measured data is shown with symbols. The absorption coefficient expected for the cases of homogeneous and inhomogeneous broadening are shown with purple dotted line and red solid line, respectively. The input wavelength is **b** 1540 nm and **c** 1565 nm

significantly when the input power is increased. Subsequently, the value flattens out at higher input powers (to the value α_{NS}). It is also apparent from the figure that the value of α in EDF at lower wavelengths is greater than its value at higher wavelengths at low input powers, for the wavelength range studied here. This is expected from its wavelength dependent absorption (Desurvire 2002). The value of α_{NS}, however, seems to be less dependent on the wavelength and is a constant value reached asymptotically at higher powers for all the wavelengths.

We analyse the trend seen in this measurement with the trend of the absorption coefficient expected for homogeneously and inhomogeneously broadened systems, given in Eqs. 1, 2 earlier. For modelling the absorption coefficient in these two cases with the help of their characteristic equations, we require the values of parameters such as α_o, P_{sat} and α_{NS}, and these are extracted from the experimental data. For this comparison, we assume $P_{sat} = P'_{sat}$. Figure 1b, c depicts the extent of the fit in the two cases at the two extreme wavelengths of 1540 nm and 1565 nm, respectively, in our measurement range. At both these wavelengths (and all the intermediate wavelengths not shown here), a perfect match is obtained between the experimentally obtained absorption coefficient (symbols) and the absorption coefficient expected for a homogeneously broadened system (dotted line) throughout the input power range of − 30 dBm to + 15 dBm. We note that at very low input powers, the absorption coefficient from the experimental data, as well as that due to homogeneous and inhomogeneous broadening are all comparable. But, as the input power increases, the experimental data match perfectly well only with the homogeneous case. This is true for all the wavelengths in the range studied here (1540–1565 nm) though this is depicted only at two wavelengths

in Fig. 1b, c. It is clear that 1 m length of EDF is following the saturable absorption expected for a homogeneously broadened system.

3.2 Long length of EDF

To know if the EDF length plays a role in the type of saturable absorption, we consider the measured data for the absorption coefficient from 25 m long EDF. Figure 2 presents the values of absorption coefficient obtained with the same experimental setup as shown in Fig. 1a but with a 25 m long EDF, for several input wavelengths in the range of 1540–1565 nm. Very low input powers are not useful here as the long length of EDF results in an unreliably low transmitted power for them. Even though the absorption coefficient as a function of input power in Fig. 2 shows the trend expected for saturable absorption, there are differences with the results seen with the 1 m long EDF in Fig. 1b, c. The value of small-signal α has reduced considerably at all the wavelengths. The slope of the curves is more during the decrease with increasing input power. The effect of changing the input wavelength is not significant for the wavelength range of 1540–1555 nm as the value of α is almost the same for this range. This is a consequence of the longer length of EDF as this was not observed in the case of 1 m (not shown here).

To analyze further for the long length of EDF, we again fit the experimentally measured data with the absorption coefficient expected for the cases of homogeneous and inhomogeneous broadening. Figure 3 illustrates this dependence. Unlike the case of 1 m EDF, the experimental data of the absorption coefficient for 25 m EDF does not match with the homogeneous case for any power range. It does not match fully with the inhomogeneous case too; rather the trend lies somewhere in between the two cases. The trend of reduction seen in the experimental data shows a sharper slope even after taking the P_{sat} values in all the three cases (symbols, dotted line, and solid line) to be the same. Hence, it leads us to the following observations: longer length of EDF is neither homogeneously nor inhomogeneously broadened over the entire power range studied here; the type of saturation may change with the input power range; and/or the presence of mixed broadening may require a change in the equation governing the saturation process. Many earlier reports mention EDF to be a homogeneous medium at room temperature for lengths such as 2.6–12 m (Bing

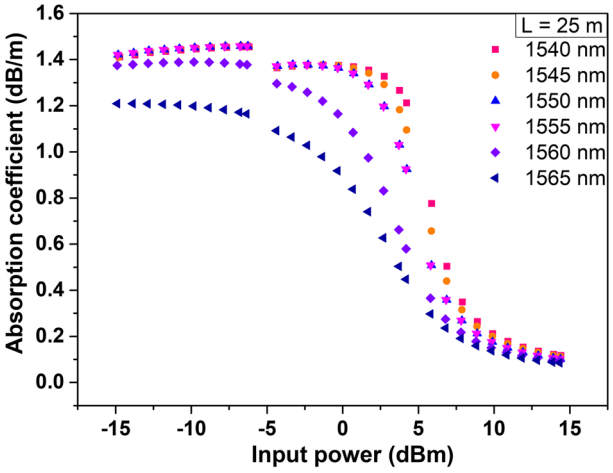

Fig. 2 Absorption coefficient obtained from output power measurements as a function of input power. Output power is measured with a power meter. EDF length is 25 m

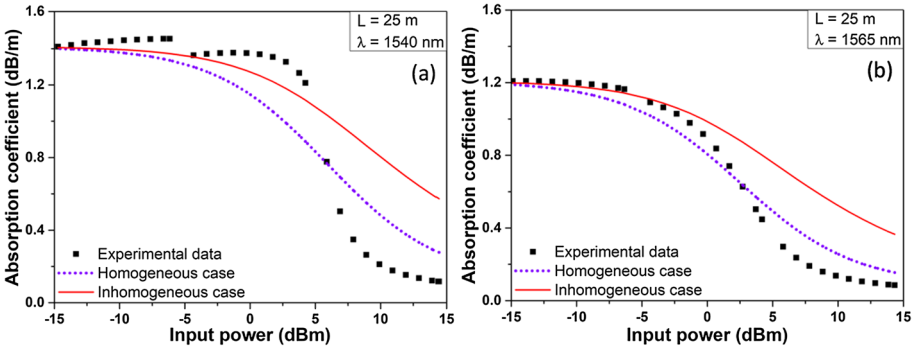

Fig. 3 Experimentally obtained absorption coefficient is shown with black square symbols, along with the absorption coefficients generated for the cases of saturation of homogeneous (purple dotted line) and inhomogeneous (red solid line) broadening, for input wavelength of **a** 1540 nm and **b** 1565 nm, for 25 m EDF. (Color figure online)

et al. 2019; Desurvire et al. 1990; Wang et al. 2013; Zhang et al. 2013). Our results for 1 m EDF support this. But this is clearly not the case for longer lengths such as 25 m used in our work. Considering the result seen in our work, it appears essential to modify the equation governing saturable absorption characteristics when working with longer lengths of EDF. In the next section, we will analyze the results from different lengths of EDF for their saturable absorption characteristics at different input wavelengths.

3.3 Modification of the characteristic equation for longer lengths of EDF

If a medium has linear optical characteristics, the basic properties of the medium such as its absorption coefficient or absorption spectrum remain unchanged even when the length of propagation of light in the medium is increased. But for EDF with the nonlinear optical property of saturable absorption, we have discussed earlier (Jachpure and Vijaya 2022) about how α_o and P_{sat} are modified at different lengths. Now, with the results in Figs. 1 and 3, it is clear that homogeneous broadening fits excellently to the saturable absorption for short lengths, but neither homogeneous nor inhomogeneous feature fits for longer lengths. In order to evaluate the required modification in the governing equation that fits the experimental data, we will first assess the impact created in the characteristic plot by changing the factors in the Eqs. 1, 2. For example, changing the P_{sat} value will shift the entire plot along the x-axis. But the value of P_{sat} cannot be changed independently as it is dependent on the values of α_o and α_{NS}. To start with, we change the exponent in the denominator of Eq. (1) and see its effects. The exponent value of 1 implies homogeneous broadening, while 0.5 refers to the inhomogeneous case (Anderson and Boffard 2017). So, we calculated the trend for different exponent values lying between 0.20 and 2.25 to extract the trend for the case of mixed broadening. In Fig. 4, we have presented the exponent value that matches the best, along with the standard cases of homogeneous and inhomogeneous broadening (dotted and solid curves respectively). This is shown for the data measured from three different EDF lengths viz., 4.6 m, 11 m, and 25 m and the two input wavelengths of 1540 nm and 1565 nm. There was no reason for the choice of these specific lengths; these are shown as they sufficiently highlight the various effects. The blue-colored star, plus and triangle

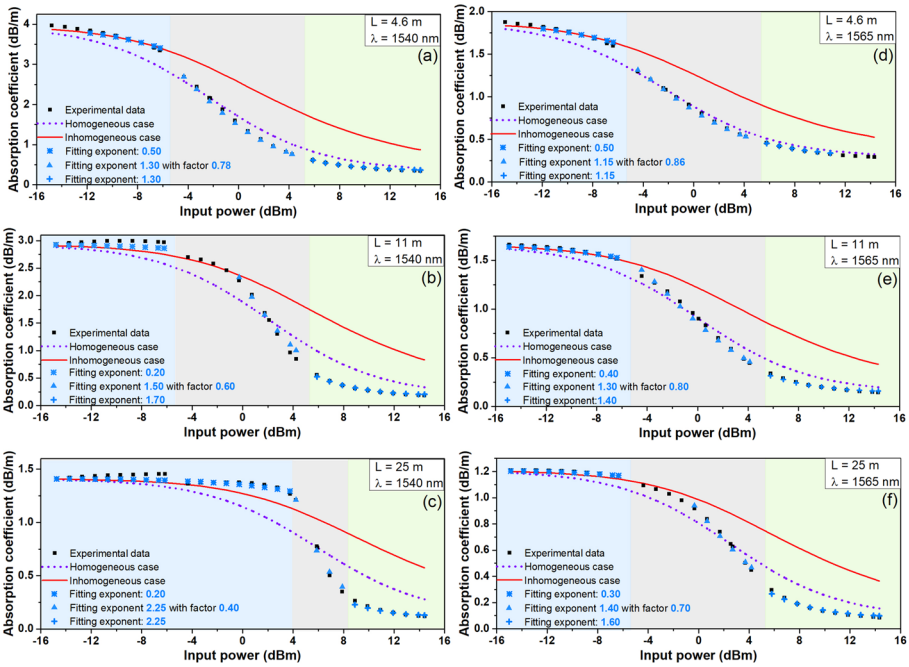

Fig. 4 Comparison of absorption coefficient in different lengths of EDF: experimental data and standard cases of homogeneous and inhomogeneous saturation cases are shown along with the best fitting exponent values at low (blue shaded region, star symbols) and high input powers (green shaded region, plus symbols) and modified exponent and factor for mid-power range (grey shaded region, triangular symbol). The EDF length is 4.6 m in (**a**) and (**d**), 11 m in (**b**) and (**e**) and 25 m in (**c**) and (**f**). The left column is for the wavelength of 1540 nm, while the right column is for 1565 nm. (Color figure onilne)

symbols in the figures show the cases where the characteristic equation with the specified exponent value matches well with the experimental data (black square symbols).

The best fitting exponent is clearly different in different cases of EDF length and wavelength. As a single value of exponent does not fit satisfactorily with the entire range of the experimental data, we have divided the range into three sections, namely Section I at very low input powers (blue shaded region), Section II for intermediate input powers near P_{sat} (grey shaded region), and Section III at the tail end of α values (green shaded region), and fitted the exponent values separately for each section. The width of the regions is not fixed prior to the fit, and is decided as appropriate for each case. For the shorter EDF length of 4.6 m (Fig. 4a, d), at lower input powers (blue shaded region), we note that the exponent value which fits best is 0.5 corresponding to the case of inhomogeneous broadening; at the higher powers (green shaded region), the best-fitting value for the exponent is higher than 1 (1.30 at 1540 nm, and 1.15 at 1565 nm). When the EDF length is increased to 11 m (Fig. 4b, e) and 25 m (Fig. 4c, f), the best-fitting exponent at lower powers reduces to 0.20 and 0.20 at the wavelength of 1540 nm, and 0.40 and 0.30 at the wavelength of 1565 nm. The best-fitting exponents at the higher power range have values of 1.70 (1540 nm) and 1.40 (1565 nm) for 11 m, and 2.25 (1540 nm) and 1.60 (1565 nm) for 25 m. For an easier comparison, these values of exponents are listed in Table 1. We conclude that the saturable absorption in EDF fits with an exponent smaller than the inhomogeneous case at lower

Table 1 List of values for the exponent in the expression for saturable absorption that fit best with the experimental data as obtained from the three sections (blue, grey, and green- shaded regions of Fig. 4) of input power variation. For section II, the value of the factor deviates from unity

Length of EDF (m)	Input wavelength (nm)	Best-fitting value of **exponent** in Section I (blue-shaded region)	Best-fitting value of **exponent** and **factor** for Section II (grey-shaded region)	Best-fitting value of **exponent** for Section III (green-shaded region)
4.6	1540	0.50	1.30, 0.78	1.30
	1565	0.50	1.15, 0.86	1.15
11.0	1540	0.20	1.50, 0.60	1.70
	1565	0.40	1.30, 0.80	1.40
25.0	1540	0.20	2.25, 0.40	2.25
	1565	0.30	1.40, 0.70	1.60

powers, while it fits with an exponent larger than the homogeneous case at higher powers, with an increase in its length. The deviation from homogeneous case is much more pronounced at the lower wavelength (1540 nm) compared to higher wavelength (1565 nm), and more pronounced for much longer lengths too, as the value of α is higher at lower wavelengths.

Similar to the lower and higher input power ranges (Sections I and III) discussed above, fitting the experimental data at the intermediate power values (Section II, grey shaded region) was also possible. But to do so, it was necessary to change the constant factor of 1 in the denominator of Eq. (1) along with the exponent value. The triangular symbols are for modifying both the exponent as well as the constant factor for this intermediate power range. As the length of EDF is increased, the modified value for the constant factor that fits the measured data at any given wavelength is reduced. As the slope in the intermediate range is steeper, a lower constant factor is required for a better fit. The constant factor is less than 1 for all the EDF lengths studied here, while being of lesser value at the lower wavelength and larger value (closer to 1) at the higher wavelength as seen in Fig. 4a–f. These are clear from the values tabulated for the three EDF lengths and two wavelengths over three different power ranges of Sections I, II and III in Table 1.

Hence, we conclude that with an EDF length of 4.6 m and lower input powers, the value of α from the experiment matches with the inhomogeneous case (best fitting exponent is 0.5). In addition, the equation for this region does not need any modification for the wavelength range of 1540–1565 nm. With the same EDF length of 4.6 m, and input powers exceeding the saturation power, the value of α from the experiment matches only with the mixed line broadening case as an exponent value more than 1 is required for the best fit; however, this value for the exponent is different for different wavelengths. For matching the trend in the measured data for the intermediate input powers for the EDF length of 4.6 m, we need to modify both the exponent and the constant factor in the denominator of Eq. (1). The results from longer lengths of 11 m and 25 m EDF indicate deviation from the homogeneous and inhomogeneous cases at all the power ranges (low, mid and high), and the deviations are much more for longer lengths. In addition, the power range corresponding to the saturation power requires change of both the exponent and the constant factor to a considerable extent (more than that for shorter length). These conclusions indicate that the inhomogeneity gets compounded in longer length of EDF. In addition, one expects intuitively that if the dimension of core is reduced, the modal qualities of the doped fiber will be affected more by the increased power per unit area, thus invoking the inhomogeneous

broadening effect at lower input power levels than in the case of larger core size. Likewise, if we change the concentration of Er-ions in the core, the magnitude of absorption coefficient and the input power levels at which saturation will occur or homogeneous/inhomogeneous effects will dominate may change; however, the conclusions drawn from the studies reported here will continue to be valid.

4 Measurement of absorption coefficient at different wavelengths in the presence of another signal at a fixed wavelength

As the emission spectrum of EDF is very broad, signals of different wavelengths can be present in the medium simultaneously either as in a multi-channel amplifier, or as in a multi-longitudinal mode laser. This can influence its properties such as its absorption coefficient at the working wavelength. In order to analyze any modification in the absorption coefficient at the working wavelength due to the presence of a signal at another wavelength in the medium, we measured α of a tunable, variable-power *probe signal*, in the presence of another lower-wavelength signal (referred to as the *saturating signal*) at two different powers. The saturating signal is at a wavelength lower than that of the probe signal, and lies closer to the centre wavelength of emission band, to ensure that downward transitions induced due to it contribute to the power measured for the probe signal. The measurement method is the same as described previously in Fig. 1a. However, as we need to provide two signals into the EDF, there is a slight modification in the experimental setup as shown in Fig. 5a. The power values recorded by the OSA here are the integrated power values (instead of the absolute power at the input wavelength) of the probe signal recorded with its spectral content at the output.

4.1 Short length of EDF

Measurement of absorption coefficient of the probe signal (at 1545 nm) in the presence of a saturating signal (at 1530 nm) is carried out initially for 1 m EDF. Figure 5b contains the measured absorption coefficient (symbols) of the probe signal both in the absence of a saturating signal and in the presence of a saturating signal (power of 0.09 mW or − 10.36 dBm). In the presence of the saturating signal at 1530 nm, the absorption experienced by the probe signal is significantly lesser than the value it would have had in the absence of that saturating signal, especially at the lower powers of − 40 to – 20 dBm. This implies that it is already saturated even at − 40 dBm of input power in this situation. Further, as its input power is increased, the absorption of the probe signal shows the characteristic saturable absorption features as in the absence of the saturating signal. The value of P_{sat} extracted from this measurement is higher in the presence of the saturating signal than the P_{sat} obtained in the absence of the saturating signal. These values are marked with two vertical lines (thick and thin respectively) for the two cases. As the probe signal power increases to that of the saturating signal power and exceeds it, the effect of the saturating signal is not present. Upon analysing its power variation with the two cases of broadening, we again found that there is perfect match of the experimentally measured data with the values generated using the equation for homogeneous saturable absorption. Hence, we conclude that the presence of a saturating signal at even a low power such as – 10 dBm can create a change in the absorption of the probe signal if it is lower in power. For the short

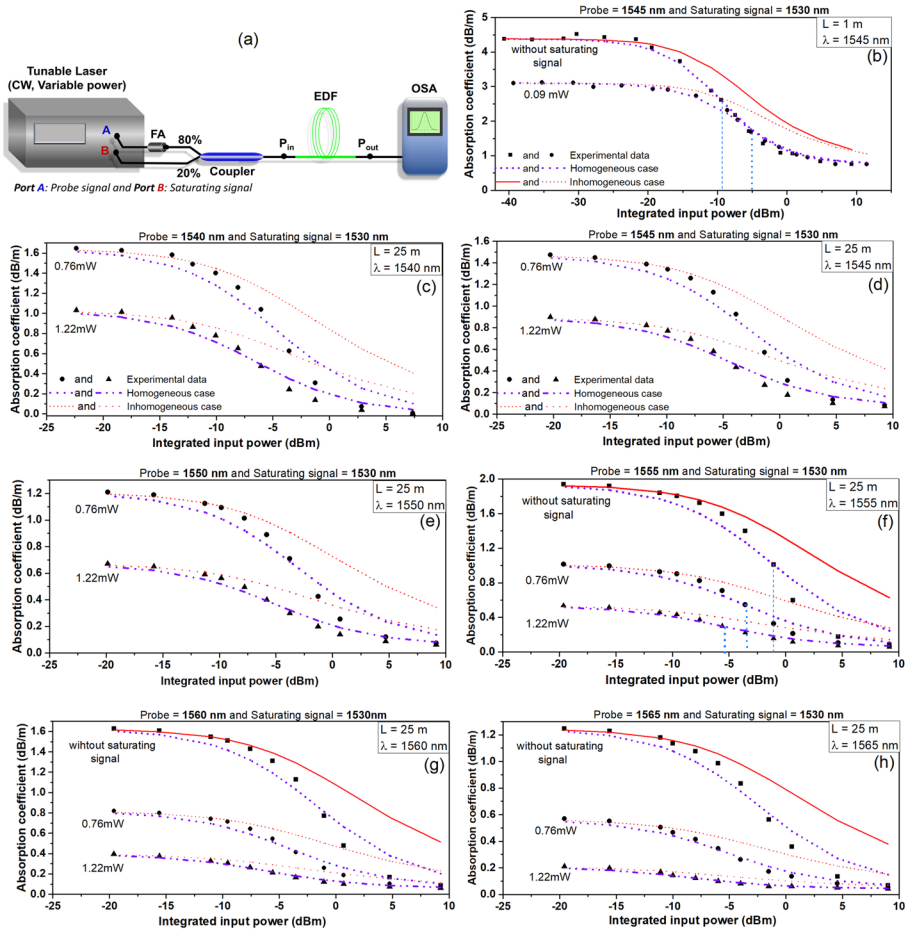

Fig. 5 **a** Experimental setup for the measurement of alpha in the presence of a saturating signal. **b** Absorption coefficient of the probe signal at 1545 nm, in the presence (power of 0.09 mW) and absence of a saturating signal (at 1530 nm) in 1 m EDF is shown; absorption coefficient of the probe signal, in the presence of a saturating signal at 1530 nm with two different powers of 0.76 mW and 1.22 mW, for 25 m long EDF is shown at probe wavelengths of **c** 1540 nm, **d** 1545 nm, **e** 1550 nm, **f** 1555 nm, **g** 1560 nm and **h** 1565 nm. The measured data is shown with symbols in (**b**–**h**). Red curve in all the plots represents the trend expected for the inhomogeneous case, and purple represents the trend for the homogeneous case. Text explains the significance of vertical lines in (**b**) and (**f**)

length of EDF, homogeneous broadening remains valid even in the presence of the saturating signal of low power.

4.2 Long length of EDF

For an EDF length of 25 m, the measured results are presented in Fig. 5c–h. The saturating signal wavelength is fixed at 1530 nm as before. The saturating signal power is set at

two fixed levels of 0.76 mW and 1.22 mW, both of which are quite small for a 25 m long EDF. The absorption characteristics of the probe signal are measured for different values of its wavelength in the range of 1540–1565 nm. The effect of the saturating signal is significant at all the probe wavelengths. The α values in the absence of the saturating signal are not shown for the probe wavelengths of 1540 nm, 1545 nm and 1550 nm (Fig. 5c–e), because the OSA was unable to detect the peak at the probe wavelength at the output of EDF due to its extremely low power (the equivalent measurement with power meter is shown in Fig. 2). But the trend in the absence of the saturating signal could be measured with the OSA at the probe wavelengths of 1555 nm, 1560 nm and 1565 nm and are shown in Fig. 5f–h. This is because the absorption loss at the larger wavelengths is lesser (Fig. 1c) and it is possible to measure the output power. It is clear that there is a large reduction (initial saturation or lowering of α_o value itself) of the absorption coefficient in the presence of the saturating signal. The extent of this reduction is not the same at the three wavelengths shown in Fig. 5f–h in the absence and presence of saturating signal power of 0.76 mW (and 1.22 mW as well). This is a signature indicative of an inhomogeneously broadened system (Anderson and Boffard 2017). In addition, if we compare the α values of the probe signal in the presence of the saturating signal powers of 0.76 mW and 1.22 mW, the initial saturation is more at the higher power of 1.22 mW. But the *change* in α between the two cases is nearly comparable in Fig. 5c–h.

Therefore, we conclude that the effect of even a small increment in the strength of the saturating signal has a significant impact on the absorption coefficient of the probe signal for longer EDF. In addition, if we compare the value of P_{sat} for 25 m (as indicated by blue vertical lines in Fig. 5f) in the absence and presence of two saturating signal powers, the value of P_{sat} extracted from the measurement is lower in the presence of the saturating signal than the P_{sat} obtained in the absence of the saturating signal. This result is the opposite of that of 1 m EDF (Fig. 5b). Hence the mechanism of saturation of absorption is different for shorter and longer lengths of EDF.

Analysing the fit of α to the homogeneous and inhomogeneous cases in the presence of the saturating signal at two different power levels, the saturated α values (with the saturating signal at a higher power of 1.22 mW) are much lower and they seem to fit better with the homogeneous case (Fig. 5c–h). This is definitely not seen in the absence of the saturating signal (Fig. 3), and in its presence if its power level is lower at 0.76 mW (Fig. 5c–h)). Thus, we conclude that the longer length of EDF is very unlike the case of shorter length (1 m) EDF even in the presence of the saturating signal. Moreover, the presence of the saturating signal reduces the small-signal absorption coefficient of the probe signal for any length of EDF. While the type of saturable absorption of shorter length EDF remains homogeneous, the saturating signal of different powers affects the type of saturable absorption of longer length EDF very differently; inhomogeneously at lower powers and homogeneously at higher powers. The inhomogeneity in longer lengths cannot be attributed to the manufacturing process as all the EDF used in this work were of commercial-grade.

The significance of this study lies where one deals with more than one signal in an amplifier system or in a laser cavity. To be specific, we can consider the optical bistability case reported earlier in (Ge et al. 2018; Li et al. 2017). There will be a broadband emission from the gain medium to start with, which will be restricted to lase at one selected wavelength chosen by the cavity filter (analogous to the probe signal in our case). There is another signal (at a different wavelength, analogous to saturating signal in our case) from an external laser to alter the output features leading to bistability. If we compare the thresholds in the absence and presence of this external signal, there is a significant reduction in threshold value in the presence of the external signal which enables one to control the

width of the bistable region. This reduction can be attributed to the fact that the absorption of the signal (set by the filter wavelength) has been reduced in the presence of an external signal in the gain medium, leading to more power in the output, and thus reducing the threshold. Similar will be the influence in amplifier systems employing the EDF, because multiple channels will not be active simultaneously at all times. The presence or absence of channels at lower wavelengths (and their combined power values) will impact the channels at higher wavelengths to a different extent depending on the length of EDF. Simple and similar gain flattening techniques will not suffice for all the EDF lengths.

5 Conclusion

We have compared the absorption coefficient measured from 1 m EDF with that from 25 m EDF by analyzing the trend at different input powers, with the two cases of saturable absorption in homogeneous and inhomogeneous broadened systems. For 1 m length, we get a perfect match between the experimentally obtained data and the homogeneous case. For 25 m, it matches neither with the homogeneous nor with the inhomogeneous case. Hence, we conclude that EDF of shorter length behaves as a homogeneously broadened medium. The longer length of EDF has a trend that lies beyond (since the modified exponent value is beyond 0.5 and 1) the two cases, necessitating a modification for the saturable absorption characteristic equation for longer lengths. This modification can be done by changing the value of the exponent and the factor 1 in the denominator of the characteristic equation. Saturable absorption data from the measurements fits well with a smaller exponent than the inhomogeneous case at lower powers, while it fits with a larger exponent than the homogeneous case at higher powers, for the case of longer length. Shorter lengths of EDF such as 1 m result in an absorption coefficient value close to the value provided by the manufacturer, which is around 5 dB/m for M-5 EDF at 1540 nm. But 25 m EDF gives the value to be around 1.4 dB/m which is considerably less. We also analysed the absorption in the presence of a saturating signal at a lower wavelength and conclude that even a very low power of the saturating signal can significantly reduce it. Interestingly, the trend expected for a homogeneously broadened system is still valid for this reduced value in 1 m EDF while there is a change in the matching trend for 25 m; with a higher saturating signal power of 1.22 mW, the match with the homogeneous case gets better than it was in its absence. All the power values used in these measurements were kept in the range often used in EDF-based amplifiers and lasers. Our work shows that some of the advantages of homogeneous and inhomogeneous broadening can be invoked with an appropriate length of EDF, suitable signal powers, choice of operating wavelength, and the presence/absence of another signal for longer lengths.

Acknowledgements The authors acknowledge useful technical discussions with Professor Utpal Das.

Author's contributions DJ and RV planned the work. DJ did all the measurements and simulations. Both DJ and RV analyzed the results and wrote the manuscript. RV supervised the work.

Funding The authors acknowledge the funding support from the Council of Scientific and Industrial Research, Govt of India (project no. 03/1514/17/EMR-II) and infrastructure support from MHRD-DRDO sponsored IMPRINT project (no. 4194).

Availability of data and materials These are available with the authors.

Declarations

Conflict of interest The authors declare no competing interests.

References

Ainslie, B.J.: A review of the fabrication and properties of erbium-doped fibers for optical amplifiers. J. Light. Technol. **9**(2), 220–227 (1991). https://doi.org/10.1109/50.65880

An, H.L., Lin, X.Z., Pun, E.Y.B., Liu, H.D.: Multi-wavelength operation of an erbium-doped fiber ring laser using a dual-pass Mach–Zehnder comb filter. Opt. Commun. **169**(1), 159–165 (1999). https://doi.org/10.1016/S0030-4018(99)00422-8

Anderson, L.W., Boffard, J.B.: Lasers for Scientists and Engineers. World Scientific Publishing Company, Singapore (2017)

Becker, P.M., Olsson, A.A., Simpson, J.R.: Erbium-Doped Fiber Amplifiers: Fundamentals and Technology. Elsevier Academic Press, San Diego (1999)

Bellemare, A.: Continuous-wave silica-based erbium-doped fibre lasers. Prog. Quantum. Electron. **27**(4), 211–266 (2003). https://doi.org/10.1016/S0079-6727(02)00025-3

Bing, F., Xuefang, Z., Zengyang, L., Yu, Z., Tianshu, W.: Experimental research on an L-band multi-wavelength erbium-doped fiber laser based on a cascaded Sagnac loop and M-Z filters. Laser Phys. **29**(6), 065102 (2019). https://doi.org/10.1088/1555-6611/ab153d

Bradley, J.D.B., Pollnau, M.: Erbium-doped integrated waveguide amplifiers and lasers. Laser Photon. Rev. **5**(3), 368–403 (2011). https://doi.org/10.1002/lpor.201000015

Cai, P., Liao, T.: Multi-wavelength fiber laser based on highly erbium-doped fiber and nonlinear effects in SMF. Optik **206**, 164257 (2020). https://doi.org/10.1016/j.ijleo.2020.164257

Casperson, L.W.: Laser broadening ratio from the multimode oscillation threshold. J. Appl. Phys. **52**(11), 6981–6983 (1981). https://doi.org/10.1063/1.328660

Casperson, L.W.: Stability criteria for lasers with mixed line broadening. Opt. Quantum Electron. **19**(1), 29–36 (1987). https://doi.org/10.1007/BF02030628

Deepa, V., Vijaya, R.: Linewidth characteristics of a filterless tunable erbium doped fiber ring laser. J. Appl. Phys. **102**(8), 083107 (2007). https://doi.org/10.1063/1.2798579

Desurvire, E.: Erbium-Doped Fiber Amplifiers: Principles and Applications. Wiley, New York (2002)

Desurvire, E., Zyskind, J.L., Simpson, J.R.: Spectral gain hole-burning at 1.53 μm in erbium-doped fiber amplifiers. IEEE Photon. Technol. Lett. **2**(4), 246–248 (1990). https://doi.org/10.1109/68.53251

Digonnet, M.J.F., Digonnet, M.J.: Rare Earth Doped Fiber Lasers and Amplifiers. CRC Press Taylor & Francis Group, Boca Raton (1993)

Flood, F.A.: Impact of pump and signal wavelength on inhomogeneous characteristics of L-Band EDFA's. Opt. Fiber Commun. Conf. (2000), Paper WG6. https://opg.optica.org/abstract.cfm?uri=OFC-2000-WG6

Ge, Q., Li, S., Wang, Z., Zhen, S., Martín, J.C., Yu, B.: Optical bistability via an external control laser in an erbium-doped-fiber laser. Opt. Laser Technol. **98**, 79–83 (2018). https://doi.org/10.1016/j.optlastec.2017.07.052

Giles, C.R., Desurvire, E.: Modeling erbium-doped fiber amplifiers. J. Light. Technol. **9**(2), 271–283 (1991). https://doi.org/10.1109/50.65886

Harun, S.W., Dimyati, K., Jayapalan, K.K., Ahmad, H.: An overview on S-band erbium-doped fiber amplifiers. Laser Phys. Lett **4**(1), 10–15 (2007). https://doi.org/10.1002/lapl.200610064

Huang, L., Yang, C., Tan, T., Lin, W., Zhang, Z., Zhou, K., Zhao, Q., Teng, X., Xu, S., Yang, Z.: Sub-kHz-linewidth wavelength-tunable single-frequency ring-cavity fiber laser for C- and L-band operation. J. Light. Technol. **39**(14), 4794–4799 (2021). https://doi.org/10.1109/JLT.2021.3074824

Ismail, A., Al-Mansoori, M., Abdullah, F., Jamaludin, M.Z., Al-Qartoubi, M., Almamari, S., Alkhaldi, H.: Tunable C + L bands triple frequency spacing multi-wavelength Brillouin-erbium fiber laser. Opt. Fiber Technol. **64**, 102535 (2021). https://doi.org/10.1016/j.yofte.2021.102535

Jachpure, D., Vijaya, R.: Saturable absorption and its consequent effects in bistable erbium-doped fiber ring laser. J. Opt. **24**(2), 024007 (2022). https://doi.org/10.1088/2040-8986/ac41d6

Kang, Q., Lim, E.-L., Jung, Y., Sahu, J.K., Poletti, F., Baskiotis, C., Alam, S., Richardson, D.J.: Accurate modal gain control in a multimode erbium doped fiber amplifier incorporating ring doping and

a simple LP_01 pump configuration. Opt. Express **20**(19), 20835 (2012). https://doi.org/10.1364/OE.20.020835

Laurent, B., Anne-Marie, J., Bernard, J., Laurent, G., Christine, M., Pascal, B., Dominique, B.: Homogeneous and inhomogeneous broadening measurements of EDFA C and L bands. Opt. Amplif. Appl. Otub1 **1**, 2 (2001). https://doi.org/10.1364/OAA.2001.OTuB1

Li, S., Ge, Q., Wang, Z., Martín, J.C., Yu, B.: Optical bistability via an external control field in all-fiber ring cavity. Sci. Rep. **7**(1), 8992 (2017). https://doi.org/10.1038/s41598-017-09570-x

Li, Y., Shen, Y., Tian, J., Fu, Q., Yao, Y.: Wavelength switchable multi-wavelength erbium-doped fiber laser based on polarization-dependent loss modulation. J. Light. Technol. **39**(1), 243–250 (2021)

Liu, Y., Sharma, M., Krol, M.F.: Dual-cavity optical gain control for EDFAs and EDFA cascades. Opt. Amplif. Appl. Tha6 **1**, 2 (1999). https://doi.org/10.1364/OAA.1999.ThA6

Mao, Q., Lit, J.W.Y.: Optical bistability in an L-band dual-wavelength erbium-doped fiber laser with overlapping cavities. IEEE Photon. Technol. Lett. **14**(9), 1252–1254 (2002). https://doi.org/10.1109/LPT.2002.801078

Siegman, E.: Lasers. University Science Books, Mill Valley (1986)

Suchita, Vijaya, R.: Temporal coherence of a low-power erbium-doped fiber laser with spectrally broadened output. J. Opt. Soc. Am. A **34**, 1004–1010 (2017). https://doi.org/10.1364/JOSAA.34.001004

Wang, P., Weng, D., Li, K., Liu, Y., Yu, X., Zhou, X.: Multi-wavelength Erbium-doped fiber laser based on four-wave-mixing effect in single mode fiber and high nonlinear fiber. Opt. Express **21**(10), 12570 (2013). https://doi.org/10.1364/OE.21.012570

Zhang, C., Sun, J., Jian, S.: A new mechanism to suppress the homogeneous gain broadening for stable multi-wavelength erbium-doped fiber laser. Opt. Commun. **288**, 97–100 (2013). https://doi.org/10.1016/j.optcom.2012.10.004

Zhao, Q., Pei, L., Wang, J., Xie, Y., Ruan, Z., Zheng, J., Li, J., Ning, T.: Interval-adjustable multi-wavelength erbium-doped fiber laser with the assistance of NOLM or NALM. IEEE Access **9**, 16316–16322 (2021). https://doi.org/10.1109/ACCESS.2021.3050462

Zhou, Y., Lou, S., Tang, Z., Zhao, T., Zhang, W.: Tunable and switchable C-band and L-band multi-wavelength erbium-doped fiber laser employing a large-core fiber filter. Opt. Laser Technol. **111**, 262–270 (2019). https://doi.org/10.1016/j.optlastec.2018.09.042